

See discussions, stats, and author profiles for this publication at: <https://www.researchgate.net/publication/37424378>

# Spectroelectrochemical Studies of $\text{Ru}(\text{bpy})_3^{2+}$ at the Water/1,2-Dichloethane Interface

ARTICLE in THE JOURNAL OF PHYSICAL CHEMISTRY · JUNE 1996

Impact Factor: 2.78 · DOI: 10.1021/jp9535452 · Source: OAI

CITATIONS

35

READS

62

4 AUTHORS, INCLUDING:



Zhifeng Ding

The University of Western Ontario

123 PUBLICATIONS 3,280 CITATIONS

SEE PROFILE



Pierre-Francois Brevet

Claude Bernard University Lyon 1

173 PUBLICATIONS 2,839 CITATIONS

SEE PROFILE



Hubert H Girault

École Polytechnique Fédérale de Lausanne

556 PUBLICATIONS 13,985 CITATIONS

SEE PROFILE

# Spectroelectrochemical Studies of $\text{Ru}(\text{bpy})_3^{2+}$ at the Water/1,2-Dichloroethane Interface

Zhifeng Ding, R. Geoffrey Wellington, Pierre F. Brevet, and Hubert H. Girault\*

Laboratoire d'Electrochimie, Département de Chimie, Ecole Polytechnique Fédérale de Lausanne, CH-1015 Lausanne, Switzerland

Received: November 30, 1995; In Final Form: March 15, 1996<sup>®</sup>

The application of differential cyclic voltfluorometry in total internal reflection (TIR) geometry to the study of  $\text{Ru}(\text{bpy})_3^{2+}$  transfer at the water/1,2-dichloroethane (DCE) interface has been studied. The emission spectra of  $\text{Ru}(\text{bpy})_3^{2+}$  in bulk water, in bulk DCE, and at various applied potentials at the water/DCE interface have also been measured. Both techniques allow discrimination between  $\text{Ru}(\text{bpy})_3^{2+}$  in water and  $\text{Ru}(\text{bpy})_3^{2+}$  in DCE. Also, the quenching of the excited state of aqueous  $\text{Ru}(\text{bpy})_3^{2+}$ , irradiated in TIR geometry, at the water/DCE interface by tetracyanoquinodimethane (TCNQ), dissolved in the adjacent organic phase, has been studied using time-resolved luminescence spectroscopy. Electrochemically controlled experiments were then conducted at applied interfacial potentials, and the only quenching observable was attributed to the transfer of  $\text{Ru}(\text{bpy})_3^{2+}$  into the DCE phase by direct comparison with the voltfluorogram measured during the same experiment. At applied potentials where  $\text{Ru}(\text{bpy})_3^{2+}$  was maintained principally in the aqueous phase, no heterogeneous electron transfer could be observed by time-resolved luminescence spectroscopy in TIR geometry.

## Introduction

The use of the liquid/liquid interface in the study of photoinduced electron transfer reactions provides the inherent advantage of product separation<sup>1–4</sup> and also provides a valuable insight into the nature of charge transfer across biological membranes.<sup>5,6</sup> Another effective and commonly used means of charge separation is microenvironments such as monolayers, polymer films, microemulsions, micelles, and others which are also based on microinterfaces.<sup>3,7,8</sup> In view of the suitability and applicability of the liquid/liquid interface, it is somewhat surprising that literature reports on electron transfer reactions are not more widespread, although several dark redox couples have been investigated.<sup>9,10,11</sup> The measurement of photocurrents associated with the quenching of the sensitizer tris(2,2'-bipyridine)ruthenium(II) ( $\text{Ru}(\text{bpy})_3^{2+}$ ), a very commonly used sensitizer in homogeneous electron transfer studies,<sup>1,2,12,13</sup> dissolved in the aqueous phase by the organic quencher heptylviologen<sup>14</sup> or tetracyanoquinodimethane (TCNQ)<sup>15</sup> dissolved in the 1,2-dichloroethane (DCE) has already been established. Photocurrents associated with the quenching of  $\text{Ru}(\text{bpy})_3^{2+}$  dissolved in the DCE phase with methylviologen ( $\text{MV}^{2+}$ ) dissolved in the aqueous phase have also been reported.<sup>16</sup> In these cases, measured photocurrents demonstrated that electron transfer, as opposed to ion transfer following a photochemical process,<sup>17</sup> does take place across the interface between two immiscible electrolyte solutions. Recently, Corn et al. have observed interfacial electron transfer reactions at the water/DCE interface using surface second harmonic generation.<sup>18</sup>

In the present paper, we apply spectroelectrochemical techniques such as total internal reflection laser-induced fluorescence and differential cyclic voltfluorometry to characterize the behavior of  $\text{Ru}(\text{bpy})_3^{2+}$  at the polarized water/1,2-dichloroethane interface.

Laser-induced fluorescence (LIF) is a well-established technique used in photochemistry to access excited state lifetimes of sensitizer molecules in bulk solution.<sup>12,13</sup> It can also give access to rates of homogeneous electron transfer reactions if

time-resolved studies are performed in the presence of a quencher. The main difficulty that arises, when interfacial reactions are studied, is the overwhelming signal produced by the molecules in the bulk of the solution as compared to those in the vicinity of the interface. Therefore, LIF, as such, offers no surface specificity for interfacial processes. On the contrary, if a total internal reflection (TIR) arrangement is used, where the incident light impinges onto the interface from the 1,2-dichloroethane (DCE) phase with an incidence angle greater than the critical angle, the transmitted light wave in the aqueous phase cannot propagate, and hence the intensity decays exponentially with the distance from the interface. As a consequence, only the  $\text{Ru}(\text{bpy})_3^{2+}$  species lying in the vicinity of the interface are excited. Luminescence studies conducted in TIR mode have already been successfully applied to the study of the rate of transfer of fluorescent ions across the liquid/liquid interface.<sup>19–22</sup> Indeed, the application of differential cyclic voltfluorometry to the  $\text{Ru}(\text{bpy})_3^{2+}$ /TCNQ system is also presented in this work and serves to highlight the enhanced sensitivity which spectroscopy offers when compared to classical electrochemical methodology.

The employment of such a technique to a specific problem, the quenching of excited aqueous  $\text{Ru}(\text{bpy})_3^{2+}$  by an organic quencher, TCNQ in DCE, is described below, and in light of previous work, some novel results have been obtained. These results show both the sensitivity and usefulness of the above techniques and highlight the advantages of such new techniques to the field of liquid/liquid electrochemistry.

## Experimental Section

**Spectroscopic Methodology.** The experimental set-up for time-resolved TIR spectroscopy<sup>23</sup> is shown schematically in Figure 1. Flash photolysis experiments were carried out with a Q-switched  $\text{Nd}^{3+}$ :YAG laser (Quanta-Ray Model 170-10) with 5-ns pulse duration and 10-Hz frequency. The third harmonic ( $\lambda = 355$  nm) with an energy of 300 mJ/pulse was used to generate within an optical parametric oscillator (OPO) (Spectra Physics, MOPO-710) monochromatic light of a chosen wavelength (in the case of  $\text{Ru}(\text{bpy})_3^{2+}$  photoexcitation, 463 nm was used). Light from the OPO was directed by optics as shown in Figure 1 through the quartz wall of the spectroelectrochemical

<sup>®</sup> Abstract published in *Advance ACS Abstracts*, June 1, 1996.

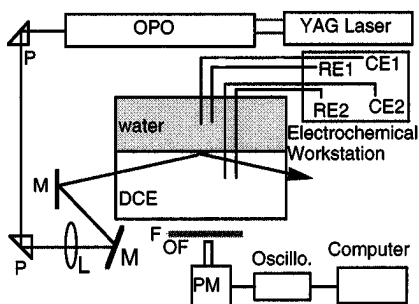


**Figure 1.** Schematic diagram showing the experimental setup employed in the potential-controlled luminescence measurements: M, mirror; P, prism; L, lens; F, filter; OF, optical fiber; RE1, RE2, Ag/AgCl or Ag/Ag<sub>2</sub>SO<sub>4</sub> reference electrodes; and CE1, CE2, platinum counter electrodes.

cell and was impinged on the interface from the DCE phase. The incidence angle to the DCE/water interface was adjusted so that the excitation beam, focused at the interface, was totally reflected. Light incident on the boundary between two non-absorbing media is reflected and refracted according to Fresnel's formula. There is no refracted beam, and the incident light is totally internally reflected for incidence angles equal to or larger than the critical angle for total reflection  $\theta_c$ , given by the following:

$$\theta_c = \sin^{-1}(n_2/n_1) \quad (1)$$

In the case of the DCE/water interface, the refractive index is greater in DCE ( $n_1 = 1.4421$ ) than in water ( $n_2 = 1.3330$ ), so the critical angle for the DCE/water interface is then 67.56° when both phases consist of pure solvents. The experiment was carried out at an incidence angle set to 75°. In this case the characteristic penetration depth  $\zeta$  is given by

$$\zeta = \frac{\lambda}{2\pi n_1 (\sin^2 \theta - n_2^2/n_1^2)^{1/2}} \quad (2)$$

where  $\lambda$  is the wavelength of the incident light,  $\theta$  is the angle of incidence, and  $n_1$  and  $n_2$  are the optical indices of the DCE and the water phase, respectively. At an angle of incidence of 75°, the penetration depth  $\zeta$  is 178 nm.

The luminescence from Ru(bpy)<sub>3</sub><sup>2+</sup> was collected through the bottom of the cell as shown in Figure 1. The luminescence was first filtered using an OG515 filter and then passed through a monochromator to a photomultiplier tube (Hamamatsu Model R928), with home-made electronics, which allowed a good response time at both high signal levels when measurements were made in bulk solution and low signal levels when measurements were taken in TIR geometry.

Time resolution was achieved with an oscilloscope (Tektronix Model TDS520A) with a high bandwidth (500 MHz), and data were downloaded to a microcomputer for further processing.

**Electrochemistry.** Electrochemical measurements were conducted using a four-electrode liquid/liquid cell of approximate interfacial area 0.9 cm<sup>2</sup> fitted with two Luggin capillaries for the reference electrodes. Photoelectrochemical and spectroelectrochemical experiments were conducted at the liquid/liquid interface by utilizing the configuration shown in Figure 2. The two aqueous electrodes are incorporated into the glass tube, and aliquots of the aqueous solution to be studied were injected by means of the attached pipet. The inclusion of an adjustable Luggin capillary for the organic phase reference electrode allowed any adverse effect of the solution resistance on the electrochemistry to be minimized. The approximate area of this interface was determined to be about 0.2 cm<sup>2</sup>.

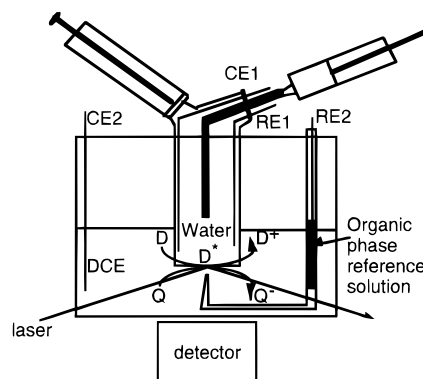
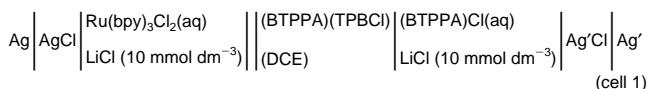


**Figure 2.** Schematic diagram showing the electrochemical/luminescence cell which was employed for these studies where RE1 and RE2 are Ag/AgCl or Ag/Ag<sub>2</sub>SO<sub>4</sub> reference electrodes and CE1 and CE2 are platinum counter electrodes.

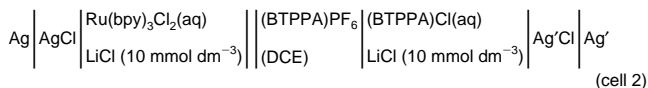
Cyclic voltammograms were recorded using a four-electrode potentiostat<sup>24</sup> which uses the positive feedback method for the compensation of the potential drop due to solution resistance. The cell chosen for determining the transfer potential of the Ru(bpy)<sub>3</sub><sup>2+</sup> was cell 1, where BTTPA represents bis(triphen-



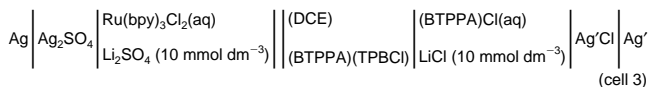
ylphosphoranylidene)ammonium and TPBCl represents tetrakis-(4-chlorophenyl)borate. The output of the potentiostat and waveform generator used to supply the voltage input were fed into a digitizer.

Using this combined spectroelectrochemical setup, the data acquisition program allowed the straightforward measurement of the emission spectrum, the signal intensity, the excited state lifetime, and the photocurrent independently at any given applied interfacial potential.

To assess any photochemical effect associated with photochemical oxidation of TPBCl<sup>-</sup> by TCNQ, cell 2 was also employed. The counter electrodes were fabricated from platinum wire; the reference electrodes were silver/silver chloride electrodes in both cell 1 and cell 2.



For certain measurements, it was instructive to extend the potential window available during the experiment, and for this reason cell 3 was chosen, since the SO<sub>4</sub><sup>2-</sup> transfers at a significantly more negative interfacial potential than Cl<sup>-</sup>.



Addition of substances to the organic phase was accomplished by means of direct injection by micropipet, followed by removal of an identical volume of the organic solution to maintain a constant height of the interface from the bottom of the cell. All solutions used were deaerated by purging with a stream of solvent-saturated nitrogen prior to use.

**Chemicals.** (BTTPA)PF<sub>6</sub> was prepared by metathesis from (BTTPA)Cl and KPF<sub>6</sub> in a 2:1 mixture of methanol and water and recrystallized in acetone. Ru(bpy)<sub>3</sub>(PF<sub>6</sub>)<sub>2</sub> was prepared in the same way from Ru(bpy)<sub>3</sub>Cl<sub>2</sub> and KPF<sub>6</sub> in water. Water was purified by reverse osmosis followed by ion exchange (Millipore

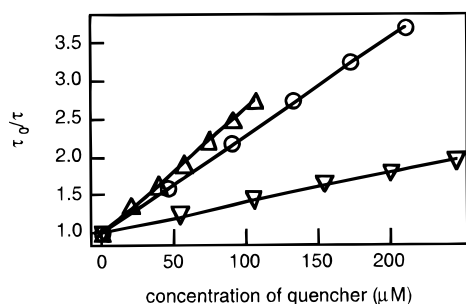


**Figure 3.** Stern–Volmer plots of  $\tau_0/\tau$  against quencher concentrations measured in bulk DCE solution using a  $\text{Ru}(\text{bpy})_3^{2+}$  concentration of  $3.28 \times 10^{-6}$  M. The quenchers employed were TCNQ ( $\Delta$ ), Fc ( $\circ$ ), and FcCOOH ( $\nabla$ ) in DCE.

Milli-Q SP Reagent Water System). 1,2-DCE (Merck, extra pure), MeCN (Fluka for UV spectroscopy), (BTPPA)Cl (Aldrich, 99%),  $\text{KPF}_6$  (Fluka, 98%), LiCl (Fluka, purum), TCNQ (Aldrich, 98%),  $\text{Ru}(\text{bpy})_3\text{Cl}_2 \cdot 6\text{H}_2\text{O}$  (Aldrich),  $\text{MVCl}_2$  (Fluka, 98%), ferrocene (Aldrich, 98%), and ferrocenecarboxylic acid (Aldrich, 96%) were used without further purification.

## Results and Discussion

**Laser-Induced Fluorescence Studies.** In order to verify the experimental methodology employed in this work, it was deemed necessary to begin with laser-induced fluorescence studies in bulk solution where the photophysical parameters of the molecules under investigation are well characterized.

**Bulk Water.** In aqueous solution the absorptive and emissive properties of  $\text{Ru}(\text{bpy})_3^{2+}$  have been extensively studied.<sup>1,2,12</sup> The absorption band centered at 453 nm corresponds to the metal to ligand charge transfer ( $^1\text{MLCT}$ ) which is coupled nonradiatively to a triplet state ( $^3\text{MLCT}$ ) which then decays back to the ground state by luminescent emission at 610 nm.<sup>25</sup> The exciting wavelength utilized was 463 nm, and simple excitation of an aqueous solution of  $\text{Ru}(\text{bpy})_3^{2+}$  gave rise to a measured luminescence decay time of the excited state of 584 ns in good agreement with the literature. The homogeneous quenching of the excited state in aqueous solution by the 1,1'-dimethyl-4,4'-bipyridinium dication ( $\text{MV}^{2+}$ ) was then investigated by time-resolved luminescence measurements where the decay time was observed to decrease as the concentration of the quencher was increased. Stern–Volmer plots of both the decay time and the intensity against the concentration of  $\text{MV}^{2+}$  were found to be linear and yielded a quenching rate constant of  $k_q = 8 \times 10^8 \text{ M}^{-1} \text{ s}^{-1}$ , again in good agreement with literature reports.<sup>26,27</sup> These results demonstrate the sensitivity and applicability of the time-resolved luminescence setup used.

**Bulk DCE.** In order to obtain photophysical data in 1,2-dichloroethane (DCE), the synthesis of  $\text{Ru}(\text{bpy})_3(\text{PF}_6)_2$  was necessary since the chloride salt is insoluble in DCE. Experiments were then conducted in bulk DCE, and a value of 660 ns was obtained for the decay time of the luminescent state of  $\text{Ru}(\text{bpy})_3^{2+}$  excited at 463 nm. Subsequent experiments then concentrated on the quenching of the excited state in DCE, and experiments were performed using TCNQ, ferrocene (Fc), ferrocenecarboxylic acid (FcCOOH), and tetracyanoethylene (TCNE) as quenchers. A typical example of the results obtained is shown in Figure 3 which is a Stern–Volmer plot of  $\tau_0/\tau$  against the quencher concentration for TCNQ, Fc, and FcCOOH. It can be seen from this figure that straight lines were obtained for each of the quenchers, again demonstrating the validity of the experimental setup. The insolubility in water and the very strong oxidizing properties of TCNQ make it an ideal candidate for study with aqueous  $\text{Ru}(\text{bpy})_3^{2+}$  as described below.

**TABLE 1: Excited State Lifetimes and Emission Spectrum Maxima for  $\text{Ru}(\text{bpy})_3^{2+}$  in Different Bulk Solvents**

solvent	$\tau_0$ (ns)	$\lambda_{\text{max}}$ (nm)
pure water	584	610
pure DCE	660	595
pure $\text{D}_2\text{O}$	1000	610
water-saturated DCE	575	596
DCE-saturated water	590	610
$\text{D}_2\text{O}$ -saturated DCE	678	
DCE-saturated $\text{D}_2\text{O}$	1000	610
MeCN	962	610

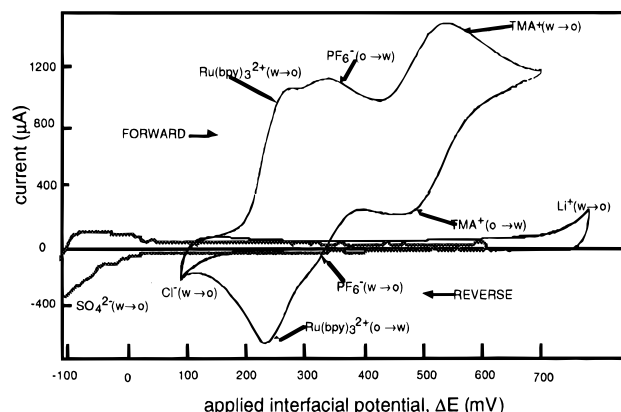
A comparison of the emission spectra of  $\text{Ru}(\text{bpy})_3^{2+}$  in water and DCE shows that the maximum in water (610 nm) is longer than in DCE (595 nm), demonstrating the greater stabilization of the excited state in the more polar aqueous medium and hence the lower transition energy back to the ground state. The lifetime of the excited state shows that the  $\text{Ru}(\text{bpy})_3^{2+}$  species decays more quickly in water (584 ns) than in DCE (660 ns). This observation can be attributed to the competition between different pathways for the relaxation of the excited state.<sup>28</sup> Water dipoles induce a faster rotational deactivation, which is an important pathway for excited state relaxation, than those of DCE and therefore lead to a shorter observed luminescence decay time.

Interestingly, if the case of  $\text{Ru}(\text{bpy})_3^{2+}$  in a water-saturated DCE solution is studied, the resultant decay lifetime (575 ns) is very close to that of pure water, demonstrating the fact that the  $\text{Ru}(\text{bpy})_3^{2+}$  maintains a first solvation shell of water molecules. The corresponding value for the decay time in DCE-saturated water was found to be 590 ns which is again characteristic of pure water. These observations therefore preclude the use of lifetime measurements to study the position of the  $\text{Ru}(\text{bpy})_3^{2+}$  species in water/DCE TIR experiments since no distinction can be made between the two solvents using this phenomenon. However, when the maximum wavelength of the emission spectrum is considered, a clear distinction can be drawn between the two solvent systems even when saturated with the other phase. For example, in the case of DCE-saturated water the measured wavelength was found to be 610 nm, identical to that of pure water. Additionally, the value for water saturated DCE solutions was found to be 596 nm, again identical to that of the pure solvent. These are relevant observations for this experimental system since the emission wavelength maximum can then be used as a criterion for measuring the position, or partitioning, of the  $\text{Ru}(\text{bpy})_3^{2+}$  species between the two solvents during the TIR experiments. All of the spectroscopic measurements conducted in bulk solvents are summarized in Tables 1 and 2, including those for heavy water ( $\text{D}_2\text{O}$ ). The  $\text{D}_2\text{O}$  results showed an identical maximum wavelength of the emission spectrum to that of water (610 nm) but a considerably longer lifetime (1000 ns), indicating that the pathways for deactivation of the excited state in  $\text{D}_2\text{O}$  are much less efficient than in either water or DCE. Another interesting observation was that mixing of  $\text{D}_2\text{O}$  and DCE together led to no difference in either the maximum wavelength of emission or the excited state lifetime of the pure solvent, indicating that in both cases the primary solvation shell remains intact.

**Electrochemical Measurements at the Water/DCE Interface.** The first set of experiments involved cyclic voltammetry at the water/DCE interface using cell 1. These measurements were conducted in order to verify the transfer potentials of the ions involved in this study. Figure 4 shows the results obtained with both  $\text{Ru}(\text{bpy})_3^{2+}$  and  $\text{PF}_6^-$  present in the system along with  $\text{TMA}^+$  added as an internal reference. It can be seen from Figure 4 that the two ions transfer at a similar transfer potential,  $\Delta\phi_{\text{water}}^{\text{DCE}}(\text{Ru}(\text{bpy})_3^{2+}) = -90 \text{ mV}$  and  $(\text{PF}_6^-) = -43 \text{ mV}$ ,

**TABLE 2: Quenching Rate Constants Obtained from Stern–Volmer Plots for  $\text{Ru}(\text{bpy})_3^{2+}$  in Different Bulk Solvents<sup>a</sup>**

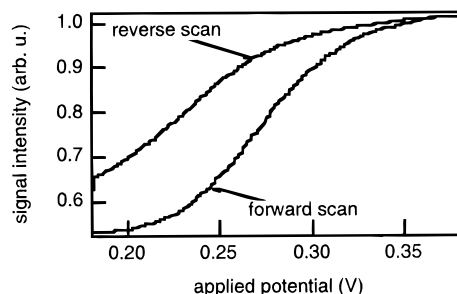
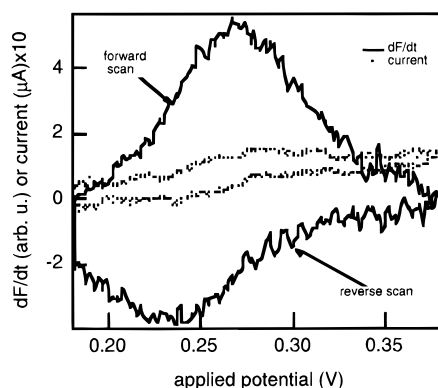
solvent	TCNQ ( $10^{10} \text{ M}^{-1} \text{ s}^{-1}$ )	$\text{MV}^{2+}$ ( $10^8 \text{ M}^{-1} \text{ s}^{-1}$ )	Fc ( $10^{10} \text{ M}^{-1} \text{ s}^{-1}$ )	FcCOOH ( $10^9 \text{ M}^{-1} \text{ s}^{-1}$ )
pure water		7.87		
pure DCE	3.60		1.37	5.13
pure $\text{D}_2\text{O}$				
water-saturated DCE	2.20			
DCE-saturated water				
$\text{D}_2\text{O}$ -saturated DCE	2.70			
DCE-saturated $\text{D}_2\text{O}$		5.56		
MeCN	3.38			

<sup>a</sup> Only a few combinations of solvents and quenchers have been used.**Figure 4.** Voltammetric response of cell 1 in both the absence and presence of  $\text{Ru}(\text{bpy})_3^{2+}$  and  $\text{PF}_6^-$ . The addition of  $\text{TMA}^+$  served as an internal reference for the system. The scan rate in both cases is 20 mV/s. The voltammetric response of cell 3 is also shown without any added  $\text{Ru}(\text{bpy})_3^{2+}$  or  $\text{PF}_6^-$  at 5 mV/s.

assuming that the standard transfer potential of the  $\text{TMA}^+$  ion is given by  $\Delta\phi_{\text{water}}^{\text{DCE}}(\text{TMA}^+) = +160 \text{ mV}$ . As the potential of the water phase becomes more positive, the transfer of  $\text{Ru}(\text{bpy})_3^{2+}$  from water to DCE can be seen along with the transfer of  $\text{PF}_6^-$  from DCE to water. Several experiments involved  $\text{PF}_6^-$  in place of the  $\text{TPBCl}^-$  anion in order to establish the photosensitivity of the  $\text{TPBCl}^-$  anion and hence its suitability for use in photochemical experiments since the  $\text{PF}_6^-$  was shown to be photochemically insensitive. Also shown in Figure 4 is the potential window measured for cell 3 where the potential window is limited by transfer of the  $\text{SO}_4^{2-}$  ion instead of the  $\text{Cl}^-$  ion and which consequently allows spectroscopic measurements over a wider range of applied potential.

**Differential Cyclic Voltfluorometry.** The inherent advantages of laser spectroscopy for bulk studies, namely, monochromaticity, high power, and high selectivity, can be applied to interfacial studies if the TIR mode is chosen. In this mode bulk contributions are minimized, and such methodology has already been applied to ion transfer at the liquid/liquid interface. Kakiuchi et al.<sup>19–22</sup> have pioneered the method of differential cyclic voltfluorometry to the study of ion transfer, and this technique is here applied to the study of  $\text{Ru}(\text{bpy})_3^{2+}$  transfer between water and DCE.

The differential cyclic voltammetric experiments employed cell 3 with a concentration of  $\text{Ru}(\text{bpy})_3^{2+}$  of  $10 \mu\text{M}$  and with the laser, operating in TIR mode, set to 463 nm. Figure 5 shows the variation of signal intensity as the applied interfacial potential is scanned from 180 mV to a switching potential of 380 mV and back to 180 mV at a scan rate of 2 mV/s. The increase in measured luminescence signal arises from the total concentration of  $\text{Ru}(\text{bpy})_3^{2+}$  which has transferred into the DCE phase since the light path for the laser light to the interface passes through the DCE solution. In order to allow the resolution of the differential cyclic voltammogram, the raw signal intensity data

**Figure 5.** Voltfluorogram recorded at a scan rate of 2 mV/s using cell 3 with a  $10 \mu\text{M}$   $\text{Ru}(\text{bpy})_3^{2+}$  concentration.**Figure 6.** Differential cyclic voltfluorogram obtained by differentiating the voltfluorogram of Figure 5 with respect to time. The corresponding electrochemical response at a scan rate of 2 mV/s is also shown for a  $10 \mu\text{M}$   $\text{Ru}(\text{bpy})_3^{2+}$  concentration.

must be differentiated with respect to time in order to obtain a signal proportional to the current density associated with the ion transfer reaction. The raw data were also smoothed using a Savitsky–Golay algorithmic smoothing procedure before differentiation although no background subtraction of the signal arising from the bulk water was necessary. The differential cyclic voltammogram obtained is shown in Figure 6, and the transfer of the fluorescent  $\text{Ru}(\text{bpy})_3^{2+}$  species can be clearly seen. The shape is, as expected, characteristic of an electrochemical voltammogram. Also shown in Figure 6 is the corresponding electrochemical response obtained simultaneously with the signal intensity data. It is clear from this figure that the transfer of the  $\text{Ru}(\text{bpy})_3^{2+}$  species at this micromolar concentration is practically invisible electrochemically, although, in contrast, it is observable from the luminescence measurement.

Additionally, in Figure 7 the electrochemical and differential cyclic voltammograms are shown for cell 2 where the background electrolyte anion in the DCE is  $\text{PF}_6^-$  in place of  $\text{TPBCl}^-$ . From this figure, it can be seen that electrochemically the transfer of  $\text{Ru}(\text{bpy})_3^{2+}$  is masked by the  $\text{PF}_6^-$  whereas the voltfluorogram clearly shows the ion transfer, indicating the usefulness of the voltfluorometric technique in studying fluorescent ions which are potential window-limiting species.<sup>19–22</sup>

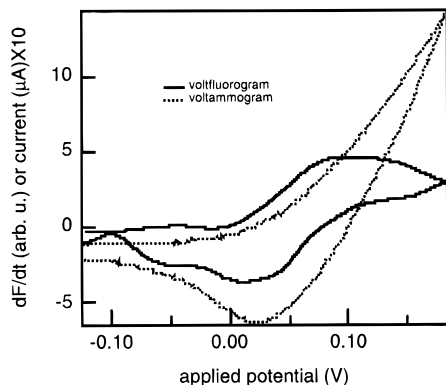


**Figure 7.** Differential cyclic voltfluorogram and the corresponding cyclic voltammogram measured at a scan rate of 2 mV/s using cell 2 with a 200  $\mu\text{M}$   $\text{Ru}(\text{bpy})_3^{2+}$  concentration.

This sensitivity of laser-induced fluorescence spectroscopy allied with the complete specificity of the measurement shows the high sensitivity of the technique to the transfer of the  $\text{Ru}(\text{bpy})_3^{2+}$  species across the interface. Since in this system only the  $\text{Ru}(\text{bpy})_3^{2+}$  is luminescent at the chosen excitation wavelength, the signal intensity arises completely from the ion of interest. In contrast, the electrochemical measurements give only a current and thus allow very limited information on the origin of this current and hence on the character of the transferring species. The differential cyclic voltfluorometry not only allows the accurate measurement of ion transfer at extremely low concentrations but also allows confidence in ensuring that the DCE has remained practically  $\text{Ru}(\text{bpy})_3^{2+}$  free and therefore that troublesome homogeneous reactions are eliminated. Clearly, the results obtained from the voltfluorometry suggest very strongly that bulk water provides only a minor contribution to the overall luminescence signal since a large difference was observed in signal intensity when the potential was swept and also since no background signal subtraction was necessary.

**Emission Spectrum Studies.** It was shown earlier that the lifetime of the excited state was not a useful criterion to determine the partitioning of the  $\text{Ru}(\text{bpy})_3^{2+}$  species but that the luminescence emission spectrum is different between the two solvents. The emission maximum in water was determined as 610 nm, whereas in DCE it was found to be 596 nm. In TIR studies, therefore, determining the emission spectrum maximum should provide another way of calculating the partitioning of the luminescent  $\text{Ru}(\text{bpy})_3^{2+}$ . However, if bulk water provides too great a contribution to the observed emission, then the measured maximum would vary little from 610 nm during TIR experiments even if the applied potential was set at a value where  $\text{Ru}(\text{bpy})_3^{2+}$  transfer was significant.

Using cell 2, the emission spectrum was measured for the  $\text{Ru}(\text{bpy})_3^{2+}$  species at a concentration of 0.2 mM, excited at 463 nm at two different applied potentials. At +180 mV,  $\text{Ru}(\text{bpy})_3^{2+}$  should exist predominantly in the aqueous phase and hence have a maximum emission of 610 nm whereas at +233 mV a significant transfer into the DCE phase should have occurred. Since the laser is incident at the interface from the DCE phase, the maximum should be closer to the one in bulk DCE, namely, 596 nm. Figure 8 shows the resultant emission spectra measured, and it is seen that a clear distinction can be made between the spectra at the two different potentials, maxima at 610 and 596 nm, respectively, being exhibited. This demonstrates that the emission spectrum maximum can be used as a criterion for showing ion transfer and also that the contribution of the bulk water does not overwhelm the measured signal. It can also be observed from Figure 8 that there is an

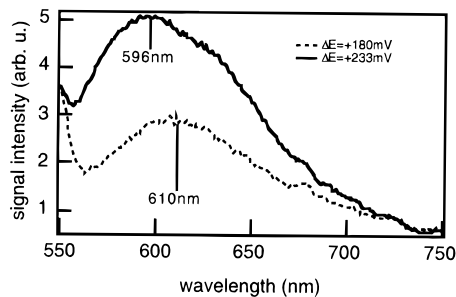


**Figure 8.** Emission spectra of a 200  $\mu\text{M}$   $\text{Ru}(\text{bpy})_3^{2+}$  concentration, excited at 463 nm in TIR mode at the water/DCE interface using cell 3. The potential applied during the measurement of each spectrum is shown on the graph.

increase in the signal intensity at +233 mV which is expected since the concentration of  $\text{Ru}(\text{bpy})_3^{2+}$  in the DCE has increased. Since the laser light is incident through the DCE phase, the contribution to the overall signal intensity from this phase is very large, and hence the experiment is very sensitive to the presence of any  $\text{Ru}(\text{bpy})_3^{2+}$  within the DCE phase. It can also be seen that at +233 mV the spectrum consists of two components. The major component arises from the  $\text{Ru}(\text{bpy})_3^{2+}$  within the DCE, centered at 596 nm, and the minor component arises from the interfacial aqueous  $\text{Ru}(\text{bpy})_3^{2+}$ , centered at 610 nm, which forms a shoulder on the emission spectrum of the  $\text{Ru}(\text{bpy})_3^{2+}$  in DCE at this potential.

**Excited State Lifetime Studies.** Using TIR time-resolved laser-induced fluorescence, we have studied the effect of the presence of a quencher in the organic phase when  $\text{Ru}(\text{bpy})_3^{2+}$  is dissolved as an aqueous electrolyte.

The lifetime of the excited state in bulk water has already been established as 584 ns. Using the configuration shown in Figure 2, the extent of the potential window of cell 3 was first determined before addition of 1 mM  $\text{Ru}(\text{bpy})_3^{2+}$  by means of injection directly into the glass tube. The applied potential was set to -100 mV during  $\text{Ru}(\text{bpy})_3^{2+}$  addition in order to prevent  $\text{Ru}(\text{bpy})_3^{2+}$  partitioning into the DCE. The time-resolved luminescence decay of the  $\text{Ru}(\text{bpy})_3^{2+}$  triplet state excited at 463 nm was then recorded in TIR mode with the detection system set to 610 nm. From this decay curve, the lifetime of the excited state was determined by fitting a single exponential function to the curve. The lifetime obtained at -100 mV was 550 ns. Following this measurement, 0.52 mM TCNQ was then added to the DCE phase and the decay curve recorded again at -100 mV. The lifetime of the excited state upon addition of the quencher was found to be unchanged. The absence of quenching demonstrates that, under these conditions, heterogeneous electron transfer cannot be observed by this technique for this system.

The applied potential was then increased, and at each potential a series of decay curves were measured. The lifetime was calculated for each applied potential, and it was found that quenching was only observed at potentials of +110 mV and above. Figure 9 shows two typical decay curves; at a potential of -30 mV  $\text{Ru}(\text{bpy})_3^{2+}$  principally exists within the aqueous phase and can be seen to be unquenched whereas at +210 mV the transfer of  $\text{Ru}(\text{bpy})_3^{2+}$  is apparent, as is the corresponding quenching of the excited state. It was found that the excited state lifetime of the  $\text{Ru}(\text{bpy})_3^{2+}$  luminescence had dropped to 260 ns at +210 mV following the homogeneous quenching by TCNQ. A differential cyclic voltfluorogram was measured during the same experiment and is shown in Figure 10, together with the lifetime data and the electrochemical response. This figure shows that the observed quenching is homogeneous in

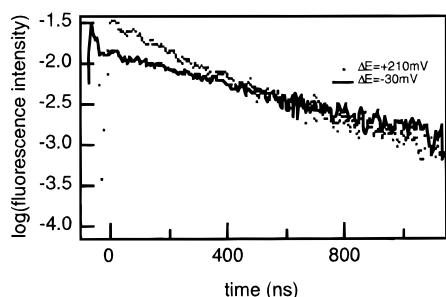


**Figure 9.** Effect of applied potential on atypical luminescence decay curves of 1 mM  $\text{Ru}(\text{bpy})_3^{2+}$  excited at 463 nm in TIR geometry using cell 3 and detected at 610 nm.

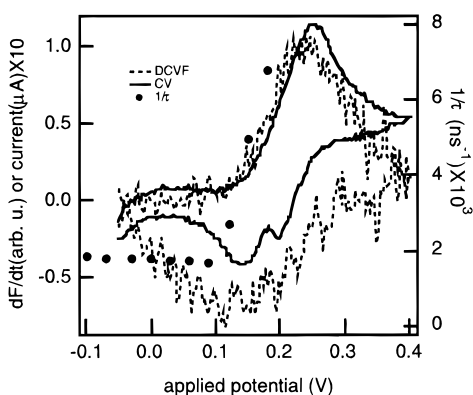


**Figure 10.** Variation of the excited state lifetime of 1 mM  $\text{Ru}(\text{bpy})_3^{2+}$  concentration excited at 463 nm using the TIR geometry as a function of applied potential with 0.74 mM TCNQ present in the DCE phase recorded at 610 nm. The corresponding differential cyclic voltfluorogram and cyclic voltammogram measured at a scan rate of 5 mV/s in cell 3 are also shown for comparison.

nature as it is exactly coincident with the onset of  $\text{Ru}(\text{bpy})_3^{2+}$  transfer into the DCE phase.

This study was conducted at several different concentrations of both  $\text{Ru}(\text{bpy})_3^{2+}$  (from 400 nM to 0.5 mM) and TCNQ (up to 5 mM), but under none of the conditions employed could the heterogeneous quenching be observed by this approach.

## Conclusions

The fluorescence properties of  $\text{Ru}(\text{bpy})_3^{2+}$  at the water/1,2-dichloroethane interface have been studied, showing in particular that the ion retains a hydration layer in the organic phase. The emission maximum was shown to be a good criterion to measure the distribution of the ion between the two phases. The technique of differential cyclic voltfluorometry has been applied to the ion transfer of  $\text{Ru}(\text{bpy})_3^{2+}$  from water to DCE and has been shown to be a sensitive method for such studies. In conjunction with this technique, time-resolved TIR luminescence

measurements at the water/DCE interface showed that only homogeneous photoinduced electron transfer between  $\text{Ru}(\text{bpy})_3^{2+}$  following the transfer from water to DCE and TCNQ in DCE could be observed. This study also demonstrates the sensitivity of the spectroscopic technique to investigate charge transfer reactions at liquid/liquid interfaces.

**Acknowledgment.** This work was supported by the European Community, Human Capital and Mobility scheme, under Grant No. CHRx-CT92-0076. Z.D. is indebted to the Commission Fédérale pour les étudiants étrangers for financial support.

## References and Notes

- (1) Atik, S. S.; Thomas, J. K. *J. Am. Chem. Soc.* **1981**, *103*, 4367, 7403.
- (2) Juris, A.; Belser, P.; von Zeelewsky, A.; Barigelletti, P.; Balzani, V. *Coord. Chem. Rev.* **1988**, *84*, 85.
- (3) Fendler, J. H. *Acc. Chem. Res.* **1980**, *13*, 7.
- (4) Kalyanasundaram, K.; Kiwi, J.; Grätzel, M. *Helv. Chim. Acta* **1978**, *61*, 2720.
- (5) Koryta, J. *Electrochim. Acta* **1979**, *24*, 293.
- (6) Benjamin, I. *Molecular Model for Electron Transfer Reaction. Structure and Reactivity in Aqueous Solution*; ACS Symposium Series 568; Washington, DC, 1994; Chapter 28.
- (7) Brugger, P. A.; Infelta, P. P.; Braun, A. M.; Grätzel, M. *J. Am. Chem. Soc.* **1981**, *103*, 320.
- (8) Sakai, K.; Muta, S.; Nagamura, T. *J. Photochem. Photobiol. A* **1995**, *87*, 151.
- (9) Samec, Z.; Marecek, V.; Weber, J.; Homolka, D. *J. Electroanal. Chem.* **1981**, *126*, 105.
- (10) Geblewicz, G.; Schiffrin, D. J. *J. Electroanal. Chem.* **1988**, *244*, 27.
- (11) Cheng, Y.; Schiffrin, D. J. *J. Chem. Soc., Faraday Trans.* **1994**, *90*, 2517.
- (12) Kalyanasundaram, K. *Coord. Chem. Rev.* **1982**, *46*, 159.
- (13) Watts, R. J. *J. Chem. Educ.* **1983**, *60*, 834.
- (14) Thomson, F. L.; Yellowlees, L. J.; Girault, H. H. *J. Chem. Soc., Chem. Commun.* **1988**, 1547.
- (15) Brown, A. R.; Yellowlees, L. J.; Girault, H. H. *J. Chem. Soc., Faraday Trans.* **1993**, *89*, 207.
- (16) Marecek, V.; De Armond, A. H.; De Armond, M. K. *J. Am. Chem. Soc.* **1989**, *111*, 2561.
- (17) Kotov, N. A.; Kuzmin, M. G. *J. Electroanal. Chem.* **1992**, *327*, 47.
- (18) Kott, K. L.; Higgins, D. A.; McMahon, R. J.; Corn, R. M. *J. Am. Chem. Soc.* **1993**, *115*, 5342.
- (19) Kakiuchi, T.; Takaso, Y.; Senda, M. *Anal. Chem.* **1992**, *64*, 3096.
- (20) Kakiuchi, T.; Takasu, Y. *Anal. Chem.* **1994**, *66*, 1853.
- (21) Kakiuchi, T.; Takasu, Y. *J. Electroanal. Chem.* **1994**, *365*, 293.
- (22) Kakiuchi, T.; Takasu, Y. *J. Electroanal. Chem.* **1995**, *381*, 5.
- (23) Toriumi, M.; Masuhara, H. *Spectrochim. Acta Rev.* **1991**, *14*, 353.
- (24) Samec, Z.; Marecek, V.; Weber, J.; Homolka, D. *J. Electroanal. Chem.* **1979**, *100*, 841.
- (25) Kober, E. M.; Meyer, T. *J. Inorg. Chem.* **1984**, *23*, 3877; **1982**, *21*, 3967.
- (26) Ochiai, E. I.; Schaffer, D. I.; Wampler, D. L.; Schettler, P. D. *Transition Met. Chem. (London)* **1986**, *11*, 241.
- (27) Kalyanasundaram, K.; Neumann-Spallart, M. *Chem. Phys. Lett.* **1982**, *88*, 7.
- (28) Rau, H.; Greiner, G. *Z. Phys. Chem.* **1991**, *170*, 73.

JP9535452